

Remote, brain-region specific control of choice behavior with ultrasonic waves

Jan Kubanek^{1*}, Julian Brown², Patrick Ye³, Kim Butts Pauly³, Tirin Moore², William Newsome²

¹Department of Biomedical Engineering, University of Utah, 36 S Wasatch Dr, Salt Lake City, UT 84112

²Department of Neurobiology, Stanford University, 318 Campus Dr, Stanford, CA 94305

³Department of Radiology, Stanford University, 1201 Welch Rd, Stanford, CA 94034

*Corresponding author

The ability to modulate neural activity in specific brain circuits remotely and systematically could revolutionize treatments of brain disorders and studies of brain function. Sound waves of high frequencies (ultrasound) have shown promise in this respect, combining the ability to modulate neuronal activity with sharp spatial focus. Here, we show that the approach can have potent effects on choice behavior. Brief, low-intensity ultrasound pulses delivered noninvasively into specific brain regions of macaque monkeys influenced their decisions regarding which target to choose. The effects were substantial, leading to around a 2 : 1 bias in choices compared to the default balanced proportion. The effect presence and polarity was controlled by the specific target region. These results represent a critical step towards the ability to influence choice behavior noninvasively and in a targeted manner. Such ability has the potential to transform the ways we treat disorders of choice and the ways we interrogate basic brain function.

Introduction

Noninvasive and reversible modulation of neuronal activity in specific brain circuits may allow us to diagnose and treat brain disorders in new, targeted ways. Low-intensity ultrasound, applied to the brain noninvasively, can be used to modulate neural activity with spatial specificity supe-

rior to other noninvasive methods such as transcranial electrical or magnetic stimulation (1–5). The neuromodulatory potential of ultrasound has been highlighted in studies that targeted perimotor regions of anesthetized rodents or rabbits. Brief, low-intensity stimuli lead to observable movements of the limbs or other body parts (6–13).

However, the enthusiasm about the neuromodulatory potential of ultrasound has recently been dampened by studies that called these effects into question (14, 15). In addition, such overt effects have not been observed in large mammals including humans. Only small changes in neural signals (16–23) or small changes in reaction time or other metrics (24–26) have been found. Yet, to make it truly useful, the approach would ideally provide neuromodulatory effects that are strong enough to manifest in behavior. For example, if clinicians are to determine which brain circuits drive a patient’s craving for an addictive drug, the neuromodulatory effects on a particular neural circuit should be potent enough to yield measurable changes in the subject’s choice behavior, i.e., whether the subject decides to use the drug or not.

Here, we engaged macaque monkeys in a choice task and report that brief pulses of low-intensity stimulation of specific brain regions have strong effects on the subjects’ choices. The ability to influence choice behavior noninvasively without using drugs could provide new ways to diagnose and treat disorders of choice.

Results

Ultrasonic control of developing decisions

We engaged two macaque monkeys in a choice task that is often used in neurology to diagnose the impact of brain lesions such as those induced by stroke (27–29). In this paradigm (Fig. 1A), one visual target is shown in the left and one in the right visual hemifield, with a short, controlled delay between the onsets. Typically, in this task, healthy, normal subjects tend to look at the target that appears first. Stroke or lesions of specific nodes of the oculomotor network, such as the frontal eye fields (FEF) or the lateral intraparietal area (LIP), strongly

affect this behavior (28–31). These oculomotor circuits preferentially represent targets in their contralateral visual hemifield (Fig. 1B). As a consequence, when neurons in these circuits are affected by a stroke, the contralateral visual hemifield is underrepresented, and subjects preferentially decide to look at the ipsilesional target (28,29). These effects are also observed for other kinds of neural perturbations, such as when neuromodulatory agents are injected into these regions. For example, when muscimol—a potent neuroinhibitory drug—is injected into left FEF of macaques (30), animals performing this task exhibit a strong ipsilateral—leftward bias (Fig. 1C, red). In contrast, injecting a drug with opposite, disinhibitory effects such as bicuculline into the same region (30) leads to an opposite, contralateral bias (Fig. 1C, blue). Analogous results are obtained for neuromodulatory interventions into area LIP (30–32). This task therefore provides a well established framework that enables us to interpret the neuromodulatory effects of ultrasound—or any other intervention, for that matter. Excitatory interventions or stimuli bias subjects’ decisions in the contralateral direction, whereas inhibitory interventions in the opposite direction.

We used this framework to evaluate the polarity and size of the effects of ultrasound on neurons (Fig. 1A). In a given session, ultrasound was applied to the animals’ left or right FEF. Ultrasound was applied in blocks of 3-6 trials and was strictly interleaved with blocks of 3-6 trials in which ultrasound was not applied to mitigate potential effects of session time. The stimulus was applied for 300 ms starting 100 ms prior to the onset of the first target to modulate neurons throughout the decision-making process. Indeed, given that animals responded on average within 171 and 263 ms (monkey A and B, respectively), this perturbation lasted long enough to influence a substantial portion of the process.

The ultrasound stimulus (Fig. 1D) had common neuromodulatory parameters (0.6 MPa, 270 kHz, 300 ms duration, 500 Hz pulse repetition frequency, 50% duty cycle). We chose a relatively low carrier frequency of 270 kHz so that we could be confident that the stimulus would effectively penetrate the animals’ skull. As a consequence, the stimulus was relatively broad as indicated by our measurements of free field pressure (Fig. 1D). Full width at half

maximum pressure was 10.5 mm in the lateral dimension and 21.8 mm in the axial direction below the skull. In monkey A (B), ultrasound was applied on average in 379 (481) trials (with a range of 103-909 (207-991)) trials per session; the stimulated trials constituted 50% of total trials.

Animals showed typical choice behavior in this task, being sensitive to the difference in target onset times (Fig. 2A, black curves). As in previous studies (28–31), the earlier a target appeared before the subsequent target, the more likely the animal was to choose that target. Critically, transcranial ultrasound had a strong influence on this choice behavior (Fig. 2A, blue curves). In the trials in which ultrasound was applied to left FEF (left column), animals were more likely to choose the rightward target. The effect reversed polarity when ultrasound was applied to right FEF (right column): in this case, animals were more likely to choose the leftward target. These single-session effects were significant ($p < 0.0017$, two-tailed two-sample proportion tests) with the exception of the monkey A left FEF example ($p = 0.074$). These examples suggest that ultrasound biases the animals' decisions in the contralateral direction.

To quantify these effects across all sessions, we measured the proportion of rightward choices in ultrasound trials at the time point at which the animals chose both targets at equal proportion when not stimulated (see Materials and Methods). We did this separately for each session (dark bars in Fig. 2B) and for data pooled over sessions (light bars in Fig. 2B). We assessed significance using a two-tailed t-test and a randomization test (see Methods), respectively. This analysis shows that targeting left FEF increased the proportion of rightward choices (Fig. 2B, left). The effect was especially strong in monkey A, who chose the rightward target, when stimulated, in 65.9% of cases at the point of otherwise equal preference (50%) when averaged over the individual sessions, and in 67.0% cases when the data of the 8 sessions were pooled together. This differed significantly from 50% across the 8 sessions in this animal ($p = 0.0015$, $t_7 = 5.0$, two-tailed t-test), as well as when the data were pooled together ($p < 0.001$, randomization test). The effect was also substantial—at about a 66% choice

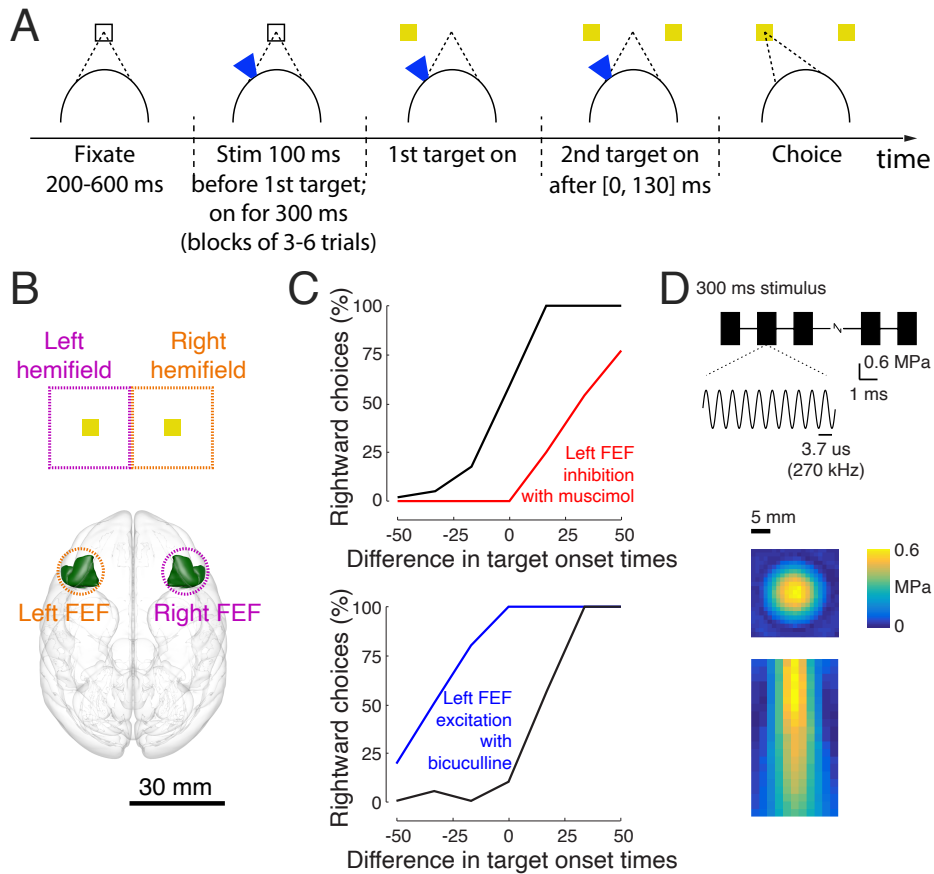


Fig. 1. Choice task and stimulus. **(A)** Task. The subject fixates a central target. One target appears in the left or the right visual hemifield. After a brief random delay, a second target appears in the opposite hemifield. The subject receives a reward for looking at either target (monkey A) or at the first target (monkey B). Ultrasound is applied in blocks of 3-6 trials, strictly interleaved with no stimulation blocks of the same duration, 100 ms prior to the appearance of the first target. **(B)** Functional characterization of the visuomotor system. We delivered the ultrasound noninvasively (intact skull and skin) into the frontal eye fields (FEF). From anatomical and functional studies, it is known that left/right FEF preferentially represents targets in the right/left visual hemifield. The outline of the FEF was rendered using the Calabrese et al. (2015) atlas with Paxinos brain regions. **(C)** Effects in previous pharmacological neuromodulation studies. When a large amount of strong inhibitory/disinhibitory drugs is injected into left FEF in this task, animals show a strong ipsilateral/contralateral bias in this task (reproduced from Schiller and Tehovnik, 2003, with permission). These results are as expected given the contralateral nature of the visual hemifield representation, and are analogous when other nodes of the visuomotor network, such as the parietal area LIP, are perturbed. **(D)** Stimulus. The ultrasound stimulus (0.6 MPa, 270 kHz, 300 ms duration) was pulsed at 500 Hz with 1 ms tone burst duration. The ultrasound was applied through a coupling cone filled with agar gel. The resulting pressure, measured in free field, is provided along the lateral (1 mm steps) and axial (2 mm steps) dimensions in color.

bias (2 : 1), the monkey chose the rightward target nearly twice as often as the leftward target. Monkey B chose the rightward target in 55.4% (average over sessions) and 55.7% (data pooled)

of cases, and this effect was significant ($p = 0.012$, $t_7 = 3.4$ and $p < 0.001$, respectively). Over the 16 sessions, the monkeys chose the rightward target at the point of equal preference in 60.7%, and this differed significantly from the 50% equal preference ($p = 0.0002$, $t_{15} = 4.9$). In 4 sessions, the effect exceeded 75% (3 : 1 choice bias). As in the single session examples (Fig. 2A, right column), the effect reversed polarity in the trials in which right FEF was stimulated (Fig. 2B, right). Monkey A chose the rightward target in 43.1% (session-average) or 45.4% (pooled) of cases. The effect was not significant when assessed over the 8 sessions, but was significant when the data were pooled together ($p = 0.0072$, randomization test). Monkey B chose the rightward target in 41.3% (42.7%) of cases, and this effect was significant ($p = 0.0024$, $t_7 = -4.6$ and $p < 0.001$, respectively). Over the 16 sessions, the monkeys chose the rightward target at the point of equal preference in 42.2% of cases, and this differed significantly from the 50% equal preference ($p = 0.00092$, $t_{15} = -4.1$). These effects are graphically summarized at the bottom of Fig. 2B. Stimulation of left FEF significantly increased the proportion of rightward choices, whereas stimulation of right FEF significantly increased the proportion of leftward choices. The contralateral nature of these shifts suggests that ultrasound positively biased the decision process represented by neurons within the stimulated region.

There was a difference in the way the two monkeys were rewarded after completing a trial. Monkey A was rewarded for choosing either target, not only for choosing the target that appeared first. This enabled the animal to choose without the guidance of target timing. A consequence was that the animal exhibited a directional bias (Fig. 2A, top row, black curves). Because such a bias is common in this task (33), to exclude its potential influence on our results, monkey B was only rewarded for choosing the first target (see Materials and Methods). This modification (31) greatly reduced this bias. Nevertheless, Fig. 2B shows that, in retrospect, this additional control was not strictly necessary—the effects point in the same direction in both animals, and are on average of comparable size.

Nature of the effect

We next investigated how rapidly the effect emerges and whether it is cumulative or, in contrast,

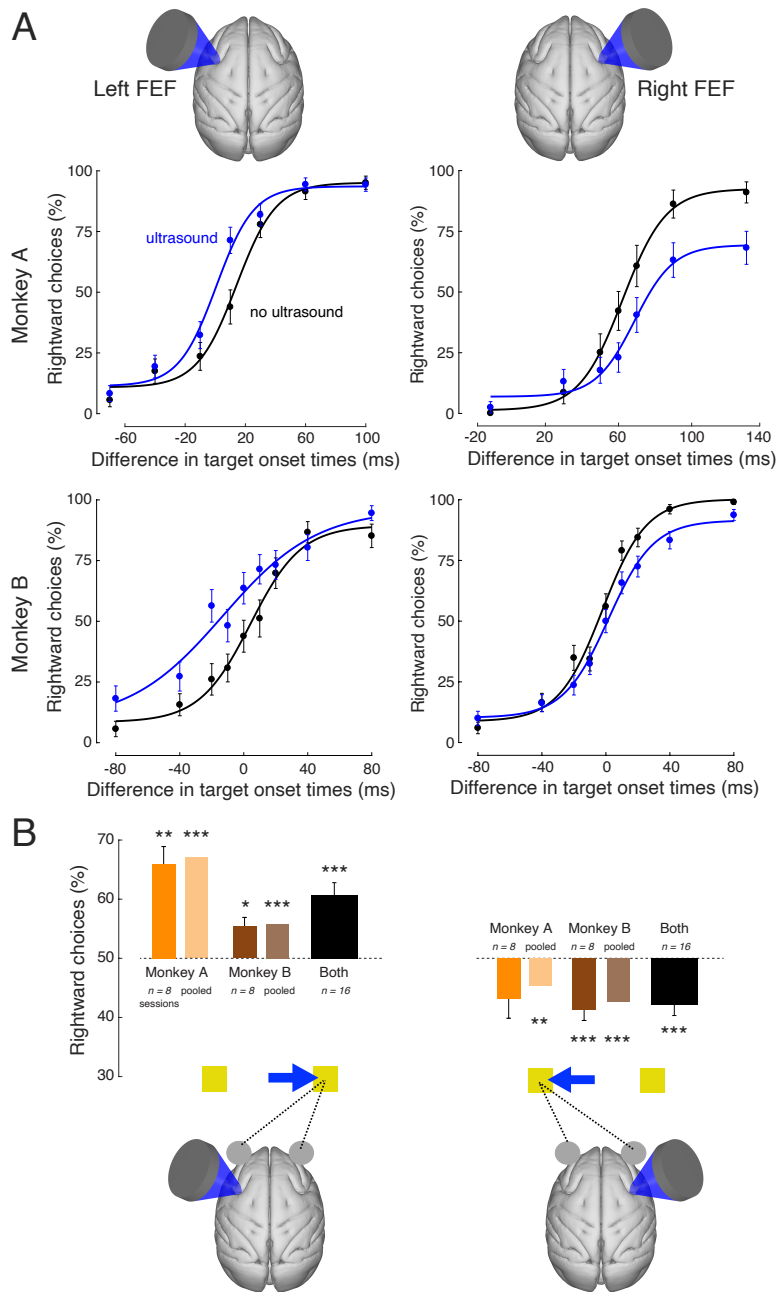


Fig. 2. Effects of ultrasonic stimulation on choice behavior. (A) Single session examples. Mean (\pm s.e.m.) proportion of choices of the rightward target as a function of the difference in target onset times. Positive difference stands for the cases in which the rightward target appeared first. The black data points reflect choice behavior in the trials in which the animal was not stimulated, whereas the blue data points represent choice behavior in the stimulated trials. The data were fit with a four-parameter sigmoid function (see Materials and Methods). The data are presented separately for left and right FEF stimulation sessions (left and right columns; see illustration on top), and for monkey A and B (top and bottom rows). (B) Quantification of the effects for all sessions. No stimulation data were fit with the sigmoid function (black curves in A). Using the fit, we identified the time difference on the abscissa for which the animal chose both targets in equal proportion (see Materials and Methods). At that point, we then assessed the proportion of rightward choices during the stimulated trials. This analysis was performed for each individual session (dark bars) and for data pooled over the sessions (light bars). The number of sessions is provided in the inset. Stars indicate the cases in which the mean effects statistically differ from equal preference (two-sided t-test for individual sessions (dark bars) and randomization test for data pooled across sessions (light bars)). *: $p < 0.05$, **: $p < 0.01$, ***: $p < 0.001$. The illustration on the bottom summarizes the polarity of the biasing effects.

whether there is an adaptation. Our task interleaves blocks of stimulated and non-stimulated trials (each 3-6 trials in duration). This block design enabled us to assess the dynamics of the ultrasonic effects as a function of the number of successively stimulated trials. To do so, we pooled data across right and left FEF stimulation sites and present the average proportion of contralateral choices as a function of trial number within a stimulated and non-stimulated block (Fig. 3A). The figure reveals that the biasing effect of ultrasound emerges immediately, in the first stimulated trial within a stimulation block, and gradually diminishes in amplitude. The effect is significant (two-tailed two-sample proportion test) in the first ($p < 0.001$), second ($p < 0.001$), third ($p = 0.010$), and fourth ($p = 0.039$) stimulated trial within a block; non-significant ($p > 0.16$) thereafter.

The analysis of Fig. 3A reveals that the choice behavior-controlling effects of ultrasound are stronger for the initial first stimuli within a stimulation block, before an adaptation occurs. Indeed, when we repeated the analysis of Fig. 2B using the first 3 trials within each stimulation block, the biasing effects of ultrasound is stronger (Fig. 3B). For instance, the effect was larger than 80% in 6 of the 16 sessions of left FEF stimulation. In these sessions, the stimulus biased the animals's choices in a ratio greater than 4 : 1. In all subsequent analyses, we use data of all trials and not only the initial stimulation trials in which the effect was strongest.

We asked whether ultrasound only biased choice or whether it, in addition, influenced perception. In particular, we asked whether ultrasound shifted the decision curves along the horizontal axis—which would represent a bias in choice, or changed the curves' slope—which would represent an impaired ability to distinguish the two targets. To do so, we fitted the decision curves with a two-parameter sigmoid fit (31), separately for the stimulated and non-stimulated decision curves within each session. We, indeed, found that ultrasound shifted the curves along the horizontal axis (Fig. 4). Left FEF stimulation shifted the decision curves on average by -7.6 ms (Fig. 4A, left), and this effect was highly significant across the sessions ($p < 0.001$, $t_{15} = -4.3$; two-sided t-test). A leftward shift indicates, for a given difference in target onset times, that the animals were more likely to choose the rightward target when

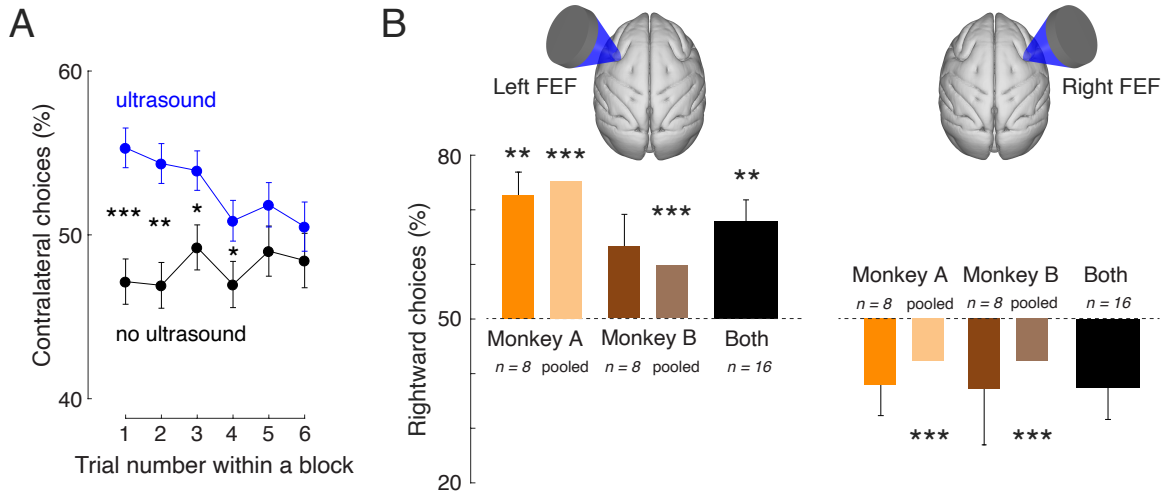


Fig. 3. The effects are stronger for initial stimuli during successive stimulation. (A) Mean \pm s.e.m. choices of the contralateral target as a function of trial number within a block, separately for non-stimulated (black) and stimulated (blue) blocks of trials. Data were pooled across left and right FEF stimulation sites. The stars indicate effect significance (two-sided two-sample proportion test; *: $p < 0.05$, **: $p < 0.01$, ***: $p < 0.001$). (B) Same format as in Fig. 2B using data of the first 3 trials of each stimulation block.

stimulated. The effect reversed polarity during right FEF stimulation, shifting the decision curves by +5.6 ms across the sessions. Also this effect was highly significant ($p = 0.0064$, $t_{15} = 3.2$). A rightward shift indicates, for a given difference in target onset times, that the animals were more likely to choose the leftward target when stimulated. These effects were significant within individual sessions (Fig. 4B). Stimulation of left FEF produced a significant horizontal shift of decision curves in 7/16 sessions, by an average of -13.4 ms (-7.6 ms across all 16 sessions). Stimulation of right FEF produced a significant horizontal shift in 3/16 sessions, by an average of $+11.1$ ms ($+5.6$ ms across all 16 sessions). These shifts corroborate the finding of Fig. 2 that ultrasound stimulation biased the animals' choices in the contralateral direction. Supplementary Figs. 1 and 2 show effects for each individual session.

Compared to the biasing effects, ultrasound had only a mild effect on the slope of the curves. Significant shallowing was observed only during left FEF stimulation (a mean change of -0.0095 ; $p = 0.032$, $t_{15} = -2.4$); not during right FEF stimulation ($p = 0.22$, $t_{15} = -1.3$). The effect was significant in only 1/16 sessions (Fig. 4B). The lack of substantial shallowing suggests that ultrasound did not notably impair the animals' ability to distinguish the onsets of

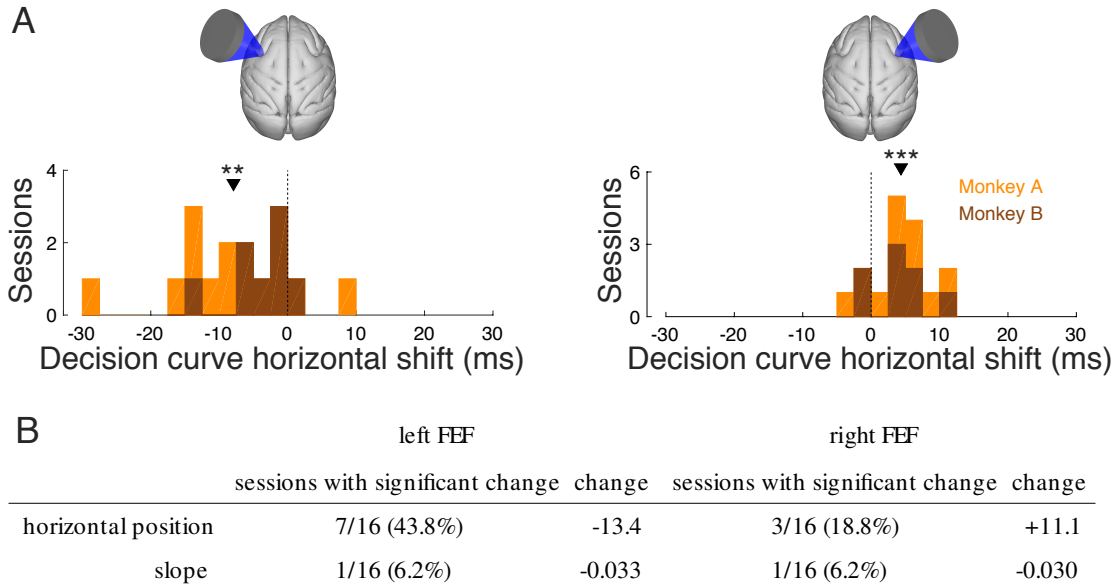


Fig. 4. Biasing nature of the effects. (A) The amount of horizontal shift of the decision curves by ultrasound (blue versus black in Fig. 2A). The data are presented separately for left and right FEF stimulation sessions (left and right panel), and separately for each session in each animal (effect histogram). The orange (brown) counts correspond to sessions of monkey A (B) and the counts are cumulative (no overlap of the orange and brown histograms). The stars indicate the effect significance (two-sided t-test; *: $p < 0.05$, **: $p < 0.01$, ***: $p < 0.001$). (B) The table shows the number of sessions (left columns) in which the parameters fitted to each decision curve (rows) changed significantly during ultrasound stimulation. See Materials and Methods for details of the statistical test. The right column shows the average magnitude of the change over the significant sessions. Horizontal position is measured in milliseconds; slope in per millisecond.

the two targets.

The effect is region-specific

A concern raised by previous studies (14, 15) is that the stimulus could be generating a radiation force whose 500 Hz modulation is audible to animals, and that this auditory perception could underlie the observed effects. This is unlikely as the differential effects of right and left FEF stimulation (Fig. 2, Fig. 4) demonstrate that the effects are specific to the stimulated regions. However, there could be a directional effect of auditory attention. To provide an additional control for such indirect confounds, we applied the same stimuli to control regions 10 mm more posterior to FEF, i.e., the motor cortex. Motor cortex is not involved in perceptual choice behavior and so in this case, there should be no effects on animals' choices. We collected data in 11 sessions of left motor cortex stimulation and 11 sessions of right motor cortex stimulation.

Besides the change in the stimulation location, data were collected in the same way as with the FEF stimulation. In contrast to FEF stimulation, motor cortex stimulation did not elicit significant biases in choice behavior (Fig. 5). There were no significant shifts from equal preference (dark bars; left motor cortex: $p = 0.43$, $t_{10} = -0.82$; right motor cortex: $p = 0.36$, $t_{10} = 0.95$). This was also the case when data over the individual sessions were pooled together (light bars; $p > 0.67$ for either monkey and hemisphere, randomization test). We further increased the power of this analysis by pooling data across left and right motor cortex stimulation sessions, thus obtaining $n = 22$ sessions. There was no significant shift from equal preference ($p = 0.63$, $t_{21} = 0.49$). We also tested for a potential reversal of effect polarity upon reversal of the stimulated hemisphere—just like we observed in FEF—by pooling positively signed left motor cortex shifts with negatively signed right motor cortex shifts. Neither this analysis yielded a significant effect ($p = 0.23$, $t_{21} = -1.24$). In addition, stimulation of left and right motor cortex did not significantly change the horizontal position or slope of the decision curves within single sessions.

Discussion

There has been considerable excitement about low-intensity ultrasound as a neuromodulatory approach because it is currently the only modality that can noninvasively target compact neural circuits, including deep nuclei, in the human brain. However, this enthusiasm has recently been curbed by studies reporting weak effects and two studies questioning the very validity of these effects (14, 15). Using non-anesthetized primates performing a choice task, we found that transcranial ultrasound can have substantial and region-specific effects on target circuits. Brief pulses of low-intensity ultrasound strongly, controllably, and reversibly influenced the subjects' choice behavior.

The effect was sizable, leading to about 2 : 1 bias in choice behavior (Fig. 2). The first initial stimuli within a stimulation block had particularly strong leverage on the choice behavior (Fig. 3), leading to up to an about 4 : 1 bias. The effect was attained using stimuli with

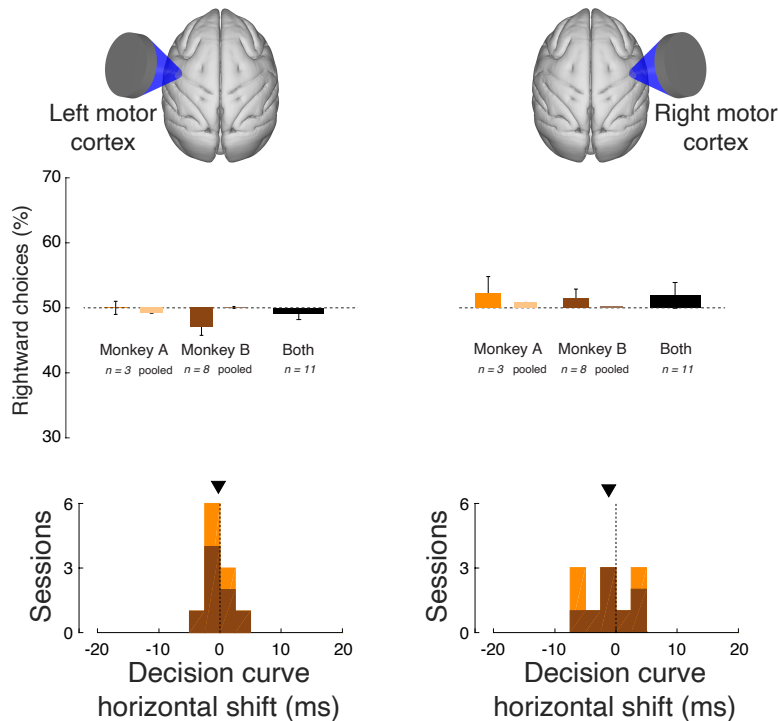


Fig. 5. Stimulation of motor cortex had no effect on choice behavior. Same format as in Fig. 2 and Fig. 4, for ultrasound stimulation of left motor cortex (left panel) and right motor cortex (right panel).

specifications that fall within the FDA guidelines on diagnostic ultrasound (see Materials and Methods) (34, 35). No adverse short- or long-term effects were observed.

Stimulation of left/right FEF shifted the animals' choices rightward/leftward (Fig. 2, Fig. 3, Fig. 4). These data suggest that our stimulus positively biased the decision process represented by neurons within the stimulated region. According to the drift-diffusion model that is often used to describe behavior in two-alternative choice tasks (see Fig. 6 for a rendering of the concept), an increase in the choice of an option could be due to three factors. First, ultrasound may bias the starting balanced state (Fig. 6, panel 1), even before a stimulus is presented. Second, ultrasound may influence the speed of the drift toward a choice (represented by a particular weight in panel 2). And finally, ultrasound may change the threshold (represented by squares of a particular height in panel 3) at which a decision is concluded. Future studies should deliver ultrasound specifically at these individual stages of the decision process to illuminate the

exact nature of the biasing effect.

The primate model, which has a sizable cranium, enabled us to investigate the local specificity of the effect. We found that mirroring the stimulation site (left versus right FEF) reversed the effect polarity. This constitutes a double dissociation of the effect through different brain regions. In addition, there were no effects when stimulating control regions that are not involved in oculomotor choice, i.e., right and left motor cortex (Fig. 5). These data provide a negative control for potential generic artifacts that can be associated with ultrasound (14, 15).

Our experimental design using blocks of sonicated trials interleaved with non-sonicated trials allowed us to assess the effect progression as a function of the number of consecutive stimuli (Fig. 3A and Supplementary Fig. 3). A neuromodulation effect can be constant in time; cumulative—increasing with each additional intervention; or diminishing—decreasing with each additional intervention. We found evidence for the latter kind. The effect emerged immediately, within the first stimulated trial. It then gradually decreased in size until becoming non-significant at 5th consecutive stimulus. This indicates that the system adapted to the repetitive stimulation. The nature of this adaptation is currently unknown. One possibility is that the adaptation occurs at the molecular level, whereby the molecular machinery gradually loses sensitivity to repetitive excitation. This possibility is likely given the emerging view that the effects of ultrasound on neurons are of a mechanical kind. In particular, the mechanical forces associated with propagating ultrasound displace membranes and this way open mechanosensitive ion channels (41–43). It has been demonstrated that mechanosensing molecular machinery adapts to repeated mechanical stimulation (44).

A previous study applied ultrasound to the FEF of macaque monkeys using an instructed antisaccade task, finding increased latency of saccades to a predefined spatial location in one condition (24). There are two fundamental differences between that and the present study. First, we used a choice task instead of an instructed task. A choice task allows us to capture and influence the process of making a decision—a higher-order cognitive process. The quality of decision-making is quantified using psychometric curves, which reveal how the decision output

(e.g., proportion of rightward choices) depends on the input decision variable (e.g., difference in target onset times). Neuromodulation-induced shifts of psychometric curves capture the effects on the neuronal pools representing each decision option (45). Neuromodulatory effects on these neuronal pools during a forming decision generally lead to substantial effects on behavior (30–32). This is because a deliberating subject has not yet committed to a specific motor output (Fig. 6). In comparison, in instructed tasks in which a subject cannot choose (24), behavioral effects are assessed using metrics of motor planning such as latency or reaction time. In such tasks, neuromodulation is less likely to manifest in behavior because the subject is committed to a specific, instructed action. Second, these studies critically differ in the timing of ultrasound application. This is important because the effects of ultrasound require appreciable time (~50-100 ms) to develop (8, 42). In (24), ultrasound was applied 100 ms after target onset. By the time ultrasound could strongly influence neurons (additional 50-100 ms), both animals in that study had already formed a plan to make a saccade, since it took them an average of 221 ms and 239 ms, respectively, from the target onset to making a saccade. Based on this timing, therefore, ultrasound could only distort the plan to make a saccade, measured as an increase in latency. In the present study, ultrasound was applied 100 ms before the onset of the first target. This early application enabled ultrasound to perturb a forming decision, thus manifesting in relatively strong behavioral effects.

This study provides several recommendations for future applications of ultrasonic neuromodulation in animals and humans. First, the effects of ultrasonic neuromodulation on behavior are likely to be maximized when a subject is making a decision. The delicate balance of weighing decision options renders neural circuitry sensitive to perturbation (Fig. 6). This has been demonstrated in previous studies (30–32) and in the present study (Fig. 2A, Supplementary Figs. 1 and 2), in which the stimulation effects are particularly prominent near the point of equal preference. Second, anesthesia should be avoided. Anesthesia dampens neuronal excitability and susceptibility to stimulation. Both the anesthesia level (48) and kind (49) affect ultrasound-mediated responses and some authors claim responses only under specific

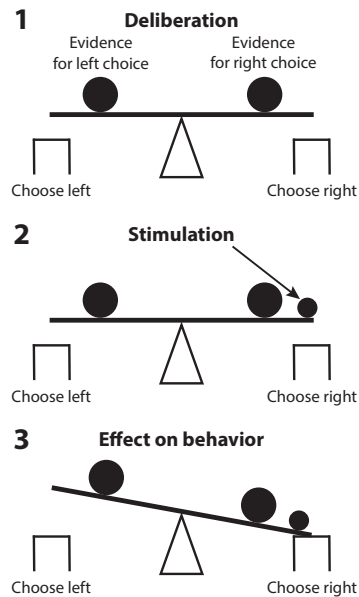


Fig. 6. Decision tasks are sensitive to neuromodulation. Decision-making renders a subject's decision system in a delicate balance between two alternatives. A relatively small perturbation (small filled circle) of the neuronal circuitry representing an alternative has a strong leverage on the subject's decision for that alternative.

anesthesia conditions (8, 11). There may even be little or no neuromodulatory effects under anesthesia (14, 15). Third, the ultrasonic stimulus should be relatively long (several dozens of milliseconds) and applied before the respective neuronal pools are engaged in a given task. This is because the effects of ultrasound take time to emerge (8, 42). This effect may be due to an integration of membrane voltage toward a threshold for activity (46). Fourth, stimulation should be applied relatively infrequently. This reflects our finding that repetitive stimulation diminishes the neuromodulatory effects (Fig. 3A and Supplementary Fig. 3). The effects of ultrasound on neurons are in part of mechanical nature (42), and it is known that frequent mechanical stimuli lead to an adaptation at the level of cells and molecules (44). And fifth, good acoustic coupling and real-time monitoring is paramount. Acoustic coupling from a transducer to skin has been in most neuromodulation studies achieved using a coupling cone. In our case, the cone was positioned over the temporal muscle. The muscle is strongly developed in male macaques and is engaged each time an animal receives juice reward. This movement could have led to a loss of coupling, or at least to variability in the targeted FEF subregions. Because specific FEF subregions code for specific target locations (47), variability in targeted FEF subregions could have led to variable effects on decision curves. Indeed, some sessions showed strong effects

and some sessions no effect, and decision curves of single sessions were affected in various ways (Supplementary Figs. 1 and 2). These methodological issues can be mitigated by using a system that i) couples ultrasound to the skin using water and ii) operates under real-time MRI guidance (39).

The finding that monkey A, who was rewarded for looking at either target, showed effects of the same polarity as monkey B suggests that ultrasound could be used to influence also internally motivated choices. This could turn ultrasound into a powerful tool to study the neural circuits involved in normal and aberrant choice behaviors. In particular, disorders of choice that include addictive, binge eating, and compulsive behaviors commonly involve deep brain regions. Selective targeting of such regions is a major strength of ultrasound (39). For instance, the nucleus accumbens shell has been causally linked with the decision whether to approach food or not in rodents (40). Ultrasound could be used to test whether this nucleus controls food intake decisions in humans. Moreover, modulation of nuclei and pathways in limbic circuits and the basal ganglia could lead to new targets for psychiatric conditions that manifest in impulsive or compulsive choices. The hardware to deliver ultrasound into the deep brain of humans is readily available and operational, attaining about a 4 mm full width at half maximum in the deep brain when using hemispherical arrays consisting of hundreds of individually controllable transducer elements (39). There are, therefore, tantalizing opportunities to apply ultrasonic neuromodulation to noninvasively modulate choice behavior in humans, with first applications aimed at determining the set of circuits involved in a given disorder in a given individual.

In summary, we investigated whether ultrasound, a pressure wave applied remotely, can modulate brain activity to an extent of producing notable effects on forming decisions. We found that brief, low-intensity ultrasonic pulses remotely delivered into oculomotor circuits of non-human primates markedly influence perceptual decisions. The presence and polarity of the effect was controllable by a specific target region. This result takes us a step closer to being able to modulate, noninvasively and reversibly, neuronal activity in specific brain circuits. This could open the way to future systematic studies of brain function in humans and to targeted,

personalized treatments of brain disorders.

Materials and Methods

Experimental Design

We trained two adult rhesus monkeys (*macaca mulatta*, monkey A: 13 kg, monkey B: 7 kg, both male) in a choice task used commonly to quantify effects of neuromodulation or neuro-intervention (27–31, 36–38). The animals sat head-fixed in a custom designed monkey chair in a completely dark room. Visual stimuli were displayed on a LCD monitor positioned 25 cm in front of the animals' eyes. Eye position was monitored using a camera (EyeLink). All procedures conformed to the Guide for the Care and Use of Laboratory Animals and were approved by Stanford University Institutional Animal Care and Use Committee. In this task, monkeys first acquired a fixation target. After a short delay, a first target (gray square of 0.5° by 0.5°) appeared in the left (right) part of the screen, 6° away from the center of fixation. After a random delay ($[0, 150]$ ms), a second target, of identical parameters, appeared in the right (left) part of the screen. The order of appearance (left versus right) was randomized from trial to trial. Once presented, both targets remained present until a choice was made. To receive a liquid reward, the animals had to make a saccade to one of the targets within 1 s after the appearance of the first target. The animal had to make the saccade within a 2° acceptance window and remain in the window for at least 100 ms. The next trial started 1.0 s following the reward delivery.

The complete a trial, monkeys were allowed to look at either target. In the first month of training, monkeys were rewarded to look at the target that appeared first. Following this initial training and during data collection, monkey A was rewarded for looking at either target. This was to allow the animal to choose without the guidance of target timing. This task led to strong directional biases over individual sessions, as reported previously (33). If a session resulted in a strong directional bias, such that the decision curve did not reach full saturation within the

used range of stimulus onset delays, we adjusted the range for the next session such that the point of equal preference lied in the middle of the range. This adjustment was only necessary for monkey A and was applied 5 times over 22 sessions. We were concerned that these biases may unpredictably interact with the stimulation effects. Therefore, in monkey B, reward was delivered only for choosing the target that appeared first. This helped to mitigate directional biases (Supplementary Fig. 2).

Ultrasonic stimulation

Ultrasound was applied in blocks of 3-6 trials (the specific number was drawn from uniform distribution bounded between 3 and 6) and was strictly interleaved with blocks of 3-6 trials in which ultrasound was not applied. We stimulated the macaque frontal eye fields (FEF) with a single-element transducer (H-115, diameter 64 mm, Sonic Concepts). The transducer was geometrically focused to 63 mm using a coupling cone filled with agar. The height of the cone was chosen such that the geometric focus was located 5 mm below the skull, to ensure that ultrasound stimulated neurons within the entire depth of the arcuate sulcus. The stimuli (270 kHz, 300 ms duration, 500 Hz pulse repetition frequency, 50% duty cycle; Fig. 1D) were generated using a commercial function generator (33520B, Keysight) and subsequently amplified using a commercial amplifier (A150, E&I). The output pressure maximum was set to 0.6 MPa. The pressure field (Fig. 1D) was characterized in vitro in free field, using Aims III (Onda) water tank filled with distilled and degassed water. The same coupling cone filled with agar gel as that used in the main experiment was used in these measurements; no ex-vivo skull was present. The measurements were taken using a calibrated fibre-optic hydrophone (Precision Acoustics). The distribution of the pressure field was measured using a robotized moving stage (Aims III) and characterized in 1 (2) mm steps in the lateral (axial) dimensions (Fig. 1D). The skull may act as an acoustic lens and so the focal area attained in the experiments may be tighter. For this stimulus, the spatial-peak pulse-average intensity in water (free field) is $I_{SPPA} = 11.6 \text{ W/cm}^2$. This value is well below the FDA track 3 recommendation of $I_{SPPA} = 190 \text{ W/cm}^2$ (34, 35). The spatial-peak time-average intensity, $I_{SPTA} = 581 \text{ mW/cm}^2$, is also below

the FDA recommendation of $I_{\text{SPTA}} = 720 \text{ mW/cm}^2$. The attenuation of the skull further lowers these values. A previous study (24) measured a pressure attenuation of $42 \pm 8\%$ through one skull; another study (19) simulated a pressure attenuation of 46% and 23% in two monkeys. Based on these data, the estimated peak pressure at focus below the skull of our animals is between 0.32 and 0.46 MPa.

During the experiment, the animals' hair was shaved and degassed ultrasound gel applied on the skin to mediate acoustic coupling between the agar-filled coupling cone and the skin. The FEF target was localized using anatomical MRI images.

Each session was conducted on a separate day; left and right stimulation sessions were also always performed on separate days.

Characterization of decision curves

We fitted the decision curves obtained in each session with a sigmoid function. The fit was performed separately for stimulated and non-stimulated data (e.g., blue and black curves in Fig. 2A). We used the same four-parameter fit as a previous study (31). This fit is mathematically equivalent to logistic fit, with the exception that it features two additional parameters to capture also vertical properties (vertical scale and vertical position) of the decision curves:

$$P(x) = \frac{1}{1 + e^{-\text{slope}(x - \text{horizpos})}} \text{vertscalescale} + \text{vertpos},$$

where $P(x)$ is the probability (frequency) of choosing the rightward target (i.e., the individual points of each decision curve), slope defines the steepness of the curve, horizpos corresponds to the position of the curve along the horizontal axis (for $\text{vertscalescale} = 1$ and $\text{vertpos} = 0$, $x = \text{horizpos}$ corresponds to the point of equal preference, i.e., the point at which a given decision curve crosses 50% of rightward choices), vertscalescale is a scaling multiplier along the vertical axis, and vertpos is a biasing term along the vertical axis.

The parameters were fitted to the choice data using non-linear minimization (function `fminsearch` in Matlab), minimizing the squared error between the fitted and the actual psychometric curves. In Fig. 4, “horizontal shift” is the difference in the fitted horizpos values of the stimulated and non-stimulated curves.

From this equation, the point of equal preference used in the analysis of Fig. 2B, Fig. 3B, and Fig. 5, x_{50} is determined as

$$x_{50} = \frac{-1}{slope} \ln \left(\frac{vertscale}{(0.5 - vertpos)} - 1 \right) + horizpos.$$

x_{50} was computed for the non-stimulated choices. Using the stimulated decision curve, we then evaluated the proportion of rightward choices $P(x_{50})$ at this point of equal preference. Fig. 2B, Fig. 3B, and Fig. 5 show the average $P(x_{50})$ across the individual sessions. In Fig. 2B and Fig. 3B, this analysis was performed for each individual session (dark bars) and for choice data pooled over the sessions (light bars). In the latter case, to assess significance, we used a randomization test, described below.

Statistical Analysis

To assess how the fitted parameters changed between stimulated and non-stimulated trials in each session (Fig. 4B), we performed a randomization test. In this test, the non-stimulated binary choice data for each difference in target onset times were sampled, with replacement, 10,000 times. Each of these re-sampled decision curves were fit with a sigmoid function. The fitting procedure was the same as above with the exception that we only used *horizpos* and *slope* as parameters. The main conclusions remain the same regardless of whether we use two or four parameters, but using two parameters helped to increase the statistical power of the analysis. The fits produced a null distribution of 10,000 values for each parameter. We then fitted the two parameters to the stimulated curve, and evaluated the probability that the parameters were drawn from the respective null distributions. If the probability was less than 0.01 for a given parameter, Bonferroni-corrected for the number of sessions, the change was considered significant.

We performed a randomization test also when assessing the significance of effects for data pooled together over the sessions. First, we determined the average point of equal preference (x_{50}) for the non-stimulated decision curve. We then sampled the binary choice data of the stimulated curve for each difference in target onset times 10,000 times, with replacement. We

computed $P(x_{50})$ for each of these 10,000 re-sampled decision curves. The test returns the probability that 0.5, i.e., equal choice proportion, was drawn from the $P(x_{50})$ distribution.

References

1. O. Naor, S. Krupa, S. Shoham, Ultrasonic neuromodulation. *Journal of Neural Engineering* **13**, 031003 (2016).
2. M. Fini, W. J. Tyler, Transcranial focused ultrasound: a new tool for non-invasive neuromodulation. *International Review of Psychiatry* **29**, 168–177 (2017).
3. J. Kubanek, Neuromodulation with transcranial focused ultrasound. *Neurosurgical focus* **44**, E14 (2018).
4. W. J. Tyler, S. W. Lani, G. M. Hwang, Ultrasonic modulation of neural circuit activity. *Current opinion in neurobiology* **50**, 222–231 (2018).
5. A. Fomenko, C. Neudorfer, R. F. Dallapiazza, S. K. Kalia, A. M. Lozano, Low-intensity ultrasound neuromodulation: An overview of mechanisms and emerging human applications. *Brain Stimulation* **11**, 1209-1217 (2018).
6. Y. Tufail, A. Yoshihiro, S. Pati, M. M. Li, W. J. Tyler, Ultrasonic neuromodulation by brain stimulation with transcranial ultrasound. *Nature Protocols* **6**, 1453–1470 (2011).
7. S.-S. Yoo, A. Bystritsky, J.-H. Lee, Y. Zhang, K. Fischer, B.-K. Min, N. J. McDannold, A. Pascual-Leone, F. A. Jolesz, Focused ultrasound modulates region-specific brain activity. *Neuroimage* **56**, 1267–1275 (2011).
8. R. L. King, J. R. Brown, W. T. Newsome, K. B. Pauly, Effective parameters for ultrasound-induced in vivo neurostimulation. *Ultrasound in Medicine & Biology* **39**, 312–331 (2013).

9. H. Kim, A. Chiu, S. D. Lee, K. Fischer, S.-S. Yoo, Focused ultrasound-mediated non-invasive brain stimulation: examination of sonication parameters. *Brain Stimulation* **7**, 748–756 (2014).
10. E. Mehić, J. M. Xu, C. J. Caler, N. K. Coulson, C. T. Moritz, P. D. Mourad, Increased anatomical specificity of neuromodulation via modulated focused ultrasound. *PLOS ONE* **9**, e86939 (2014).
11. P. P. Ye, J. R. Brown, K. B. Pauly, Frequency dependence of ultrasound neurostimulation in the mouse brain. *Ultrasound in medicine & biology* **42**, 1512–1530 (2016).
12. H. A. Kamimura, S. Wang, H. Chen, Q. Wang, C. Aurup, C. Acosta, A. A. Carneiro, E. E. Konofagou, Focused ultrasound neuromodulation of cortical and subcortical brain structures using 1.9 mhz. *Medical physics* **43**, 5730–5735 (2016).
13. G.-F. Li, H.-X. Zhao, H. Zhou, F. Yan, J.-Y. Wang, C.-X. Xu, C.-Z. Wang, L.-L. Niu, L. Meng, S. Wu, *et al.*, Improved anatomical specificity of non-invasive neuro-stimulation by high frequency (5 mhz) ultrasound. *Scientific Reports* **6**, 24738 (2016).
14. H. Guo, M. Hamilton II, S. J. Offutt, C. D. Gloeckner, T. Li, Y. Kim, W. Legon, J. K. Alford, H. H. Lim, Ultrasound produces extensive brain activation via a cochlear pathway. *Neuron* **98**, 1020–1030 (2018).
15. T. Sato, M. G. Shapiro, D. Y. Tsao, Ultrasonic neuromodulation causes widespread cortical activation via an indirect auditory mechanism. *Neuron* **98**, 1031-1041 (2018).
16. W. Legon, T. F. Sato, A. Opitz, J. Mueller, A. Barbour, A. Williams, W. J. Tyler, Transcranial focused ultrasound modulates the activity of primary somatosensory cortex in humans. *Nature Neuroscience* **17**, 322–329 (2014).

17. W. Lee, H. Kim, Y. Jung, I.-U. Song, Y. A. Chung, S.-S. Yoo, Image-guided transcranial focused ultrasound stimulates human primary somatosensory cortex. *Scientific Reports* **5**, 8743 (2015).
18. W. Lee, H.-C. Kim, Y. Jung, Y. A. Chung, I.-U. Song, J.-H. Lee, S.-S. Yoo, Transcranial focused ultrasound stimulation of human primary visual cortex. *Scientific Reports* **6**, 34026 (2016).
19. N. Wattiez, C. Constans, T. Deffieux, P. M. Daye, M. Tanter, J.-F. Aubry, P. Pouget, Transcranial ultrasonic stimulation modulates single-neuron discharge in macaques performing an antisaccade task. *Brain Stimulation* **10**, 1024–1031 (2017).
20. W. Legon, L. Ai, P. Bansal, J. K. Mueller, Neuromodulation with single-element transcranial focused ultrasound in human thalamus. *Human brain mapping* **39**, 1995–2006 (2018).
21. L. Verhagen, C. Gallea, D. Folloni, C. Constans, D. E. Jensen, H. Ahnine, L. Roumazeilles, M. Santin, B. Ahmed, S. Lehericy, *et al.*, Offline impact of transcranial focused ultrasound on cortical activation in primates. *Elife* **8**, e40541 (2019).
22. D. Folloni, L. Verhagen, R. B. Mars, E. Fouragnan, C. Constans, J.-F. Aubry, M. F. Rushworth, J. Sallet, Manipulation of subcortical and deep cortical activity in the primate brain using transcranial focused ultrasound stimulation. *Neuron* **101**, 1109–1116 (2019).
23. E. F. Fouragnan, B. K. Chau, D. Folloni, N. Kolling, L. Verhagen, M. Klein-Flügge, L. Tankelevitch, G. K. Papageorgiou, J.-F. Aubry, J. Sallet, *et al.*, The macaque anterior cingulate cortex translates counterfactual choice value into actual behavioral change. *Nature Neuroscience* **22**, 797 (2019).
24. T. Deffieux, Y. Younan, N. Wattiez, M. Tanter, P. Pouget, J.-F. Aubry, Low-intensity focused ultrasound modulates monkey visuomotor behavior. *Current Biology* **23**, 2430–2433 (2013).

25. S. Hameroff, M. Trakas, C. Duffield, E. Annabi, M. B. Gerace, P. Boyle, A. Lucas, Q. Amos, A. Buadu, J. J. Badal, Transcranial ultrasound (TUS) effects on mental states: a pilot study. *Brain Stimulation* **6**, 409–415 (2013).
26. W. Legon, P. Bansal, R. Tyshynsky, L. Ai, J. K. Mueller, Transcranial focused ultrasound neuromodulation of the human primary motor cortex. *Scientific Reports* **8** (2018).
27. H. Oppenheim, Über eine durch eine klinisch bisher nicht verwerthete Untersuchungsmethode ermittelte Form der Sensibilitätsstörung bei einseitigen Erkrankungen des Großhirns. *Neurologisches Centralblatt* **4**, 529–533 (1885).
28. C. Rorden, J. B. Mattingley, H.-O. Karnath, J. Driver, Visual extinction and prior entry: Impaired perception of temporal order with intact motion perception after unilateral parietal damage. *Neuropsychologia* **35**, 421–433 (1997).
29. T. Ro, C. Rorden, J. Driver, R. Rafal, Ipsilesional biases in saccades but not perception after lesions of the human inferior parietal lobule. *Journal of Cognitive Neuroscience* **13**, 920–929 (2001).
30. P. H. Schiller, E. J. Tehovnik, Cortical inhibitory circuits in eye-movement generation. *European Journal of Neuroscience* **18**, 3127–3133 (2003).
31. J. Kubanek, J. M. Li, L. H. Snyder, Motor role of parietal cortex in a monkey model of hemispatial neglect. *Proceedings of the National Academy of Sciences* **112**, E2067–E2072 (2015).
32. T. D. Hanks, J. Ditterich, M. N. Shadlen, Microstimulation of macaque area LIP affects decision-making in a motion discrimination task. *Nat Neurosci* **9**, 682–9 (2006).
33. B. Noudoost, T. Moore, Control of visual cortical signals by prefrontal dopamine. *Nature* **474**, 372–375 (2011).

34. K. R. Nightingale, C. C. Church, G. Harris, K. A. Wear, M. R. Bailey, P. L. Carson, H. Jiang, K. L. Sandstrom, T. L. Szabo, M. C. Ziskin, Conditionally increased acoustic pressures in nonfetal diagnostic ultrasound examinations without contrast agents: A preliminary assessment. *Journal of Ultrasound in Medicine* **34**, 1–41 (2015).
35. FDA, Marketing clearance of diagnostic ultrasound systems and transducers. *Guidance for Industry and Food and Drug Administration Staff* (2019).
36. P. H. Schiller, I.-h. Chou, The effects of frontal eye field and dorsomedial frontal cortex lesions on visually guided eye movements. *Nature Neuroscience* **1**, 248–253 (1998).
37. C. Wardak, E. Olivier, J.-R. Duhamel, Saccadic target selection deficits after lateral intraparietal area inactivation in monkeys. *The Journal of Neuroscience* **22**, 9877–9884 (2002).
38. P. F. Balan, J. Gottlieb, Functional significance of nonspatial information in monkey lateral intraparietal area. *The Journal of Neuroscience* **29**, 8166–76 (2009).
39. P. Ghanouni, K. B. Pauly, W. J. Elias, J. Henderson, J. Sheehan, S. Monteith, M. Wintermark, Transcranial MRI-guided focused ultrasound: a review of the technologic and neurologic applications. *American Journal of Roentgenology* **205**, 150–159 (2015).
40. C. H. Halpern, A. Tekriwal, J. Santollo, J. G. Keating, J. A. Wolf, D. Daniels, T. L. Bale, Amelioration of binge eating by nucleus accumbens shell deep brain stimulation in mice involves d2 receptor modulation. *Journal of Neuroscience* **33**, 7122–7129 (2013).
41. W. J. Tyler, Noninvasive neuromodulation with ultrasound? a continuum mechanics hypothesis. *The Neuroscientist* **17**, 25–36 (2011).
42. J. Kubanek, P. Shukla, A. Das, S. A. Baccus, M. B. Goodman, Ultrasound elicits behavioral responses through mechanical effects on neurons and ion channels in a simple nervous system. *Journal of Neuroscience* pp. 1458–17 (2018).

43. M. L. Prieto, K. Firouzi, B. T. Khuri-Yakub, M. Maduke, Activation of Piezo1 but not NaV1.2 channels by ultrasound at 43 MHz. *Ultrasound in medicine & biology* **44**, 1217–1232 (2018).
44. S. L. Geffeney, M. B. Goodman, How we feel: ion channel partnerships that detect mechanical inputs and give rise to touch and pain perception. *Neuron* **74**, 609–619 (2012).
45. J. I. Gold, M. N. Shadlen, The neural basis of decision making. *Annu Rev Neurosci* **30**, 535–74 (2007).
46. B. Krasovitski, V. Frenkel, S. Shoham, E. Kimmel, Intramembrane cavitation as a unifying mechanism for ultrasound-induced bioeffects. *Proceedings of the National Academy of Sciences* **108**, 3258–3263 (2011).
47. C. J. Bruce, M. E. Goldberg, M. C. Bushnell, G. B. Stanton, Primate frontal eye fields. ii. physiological and anatomical correlates of electrically evoked eye movements. *Journal of neurophysiology* **54**, 714–734 (1985).
48. Y. Younan, T. Deffieux, B. Larrat, M. Fink, M. Tanter, J.-F. Aubry, Influence of the pressure field distribution in transcranial ultrasonic neurostimulation. *Medical physics* **40**, 082902 (2013).
49. W. Lee, P. Croce, R. W. Margolin, A. Cammalleri, K. Yoon, S.-S. Yoo, Transcranial focused ultrasound stimulation of motor cortical areas in freely-moving awake rats. *BMC neuroscience* **19**, 57 (2018).

Acknowledgements

This work was supported by the NIH grant K99NS100986 (JK), Stanford Medicine Dean's Fellowship (JK), and Howard Hughes Medical Institute (JB, TM, WN). We thank Sania Fong and Shellie Hyde for technical and procedural assistance.

All data needed to evaluate the conclusions in the paper are present in the paper and the Supplementary Materials. Additional data such as saccadic traces are available from authors upon request.

J.K. designed the task, performed the experiments, analyzed the data, and wrote the paper. J.B. designed the task and edited the paper. P.Y. performed the experiments. K.B. designed the task and edited the paper. T.M. designed the task and edited the paper. B.N. designed the task and edited the paper.

The authors declare no conflicts of interest.